CAS

THE CERN ACCELERATOR SCHOOL

Maxwell's Equations for Magnets

Part II: Realistic Fields

Andy Wolski

The Cockcroft Institute, and the University of Liverpool, UK

CAS Specialised Course on Magnets
Bruges, Belgium, June 2009

In the first lecture, we saw that multipole fields of the form:

$$B_y + iB_x = C_n(x + iy)^{n-1} = C_n r^{n-1} e^{i(n-1)\theta} \tag{1}$$

with $B_z =$ constant, provided valid solutions to Maxwell's equations in free space.

We also saw that such a field could be generated by a current flowing parallel to the z-axis, on a cylinder of radius r_0, with distribution:

$$I(\theta) = I_n \cos n(\theta - \theta_n). \tag{2}$$

In this case, the field is given by:

$$B_y + iB_x = \frac{\mu_0 I_n}{2r_0} e^{-in\theta_n} \left(\frac{r}{r_0}\right)^{n-1} e^{i(n-1)\theta}. \tag{3}$$

Multipole fields can also be generated by currents flowing in wires wound around iron poles. For a pure $2n$-pole field, the shape of the surface of the iron pole must match a surface of constant scalar potential, Φ, given by:

$$\Phi = -|C_n|\frac{r^n}{n}\sin n(\theta - \theta_n). \tag{4}$$

The field is given by:

$$\vec{B} = -\nabla\Phi. \tag{5}$$

If each pole in an "ideal" $2n$-pole magnet is wound with N turns of wire carrying current I, then the multipole gradient of the field is:

$$\frac{\partial^{n-1}B_y}{\partial x^{n-1}} = \frac{n!\mu_0 NI}{r_0^n}, \tag{6}$$

where r_0 is the radius of the largest cylinder that can be inscribed between the poles.

Goals for Lecture 2

In this lecture, we shall go beyond the idealised geometries and materials that we assumed in Lecture 1, to consider more realistic magnets. In particular, we shall:

1. deduce that the symmetry of a magnet imposes constraints on the possible multipole field components, even if we relax the constraints on the material properties and other geometrical properties;

2. consider different techniques for deriving the multipole field components from measurements of the fields within a magnet;

3. discuss the solutions to Maxwell's equations that may be used for describing fields in three dimensions.

In general, from equation (1), a pure $2n$-pole field can be written:

$$B_y + iB_x = |C_n| e^{-in\theta_n} r^{n-1} e^{i(n-1)\theta}, \tag{7}$$

where r and θ are the polar coordinates within the magnet, and θ_n is the angle by which the magnet is rolled around the z axis.

We cannot design a realistic magnet to produce a pure $2n$-pole field. The materials will have finite permeability and finite dimensions, and may saturate.

More generally, a field consists of a superposition of $2n$-pole fields:

$$B_y + iB_x = \sum_{n=1}^{\infty} |C_n| e^{-in\theta_n} r^{n-1} e^{i(n-1)\theta}. \tag{8}$$

However, in the design of a $2n$-pole magnet, we *can* impose a perfect symmetry under rotations through $2\pi/n$ about the z axis.

In fact, we see from equation (7):

$$B_y + iB_x = |C_n| e^{-in\theta_n} r^{n-1} e^{i(n-1)\theta}, \tag{9}$$

that under a rotation by π/n, i.e. $\theta_n \mapsto \theta_n + \pi/n$, the field changes sign:

$$\vec{B} \mapsto -\vec{B}. \tag{10}$$

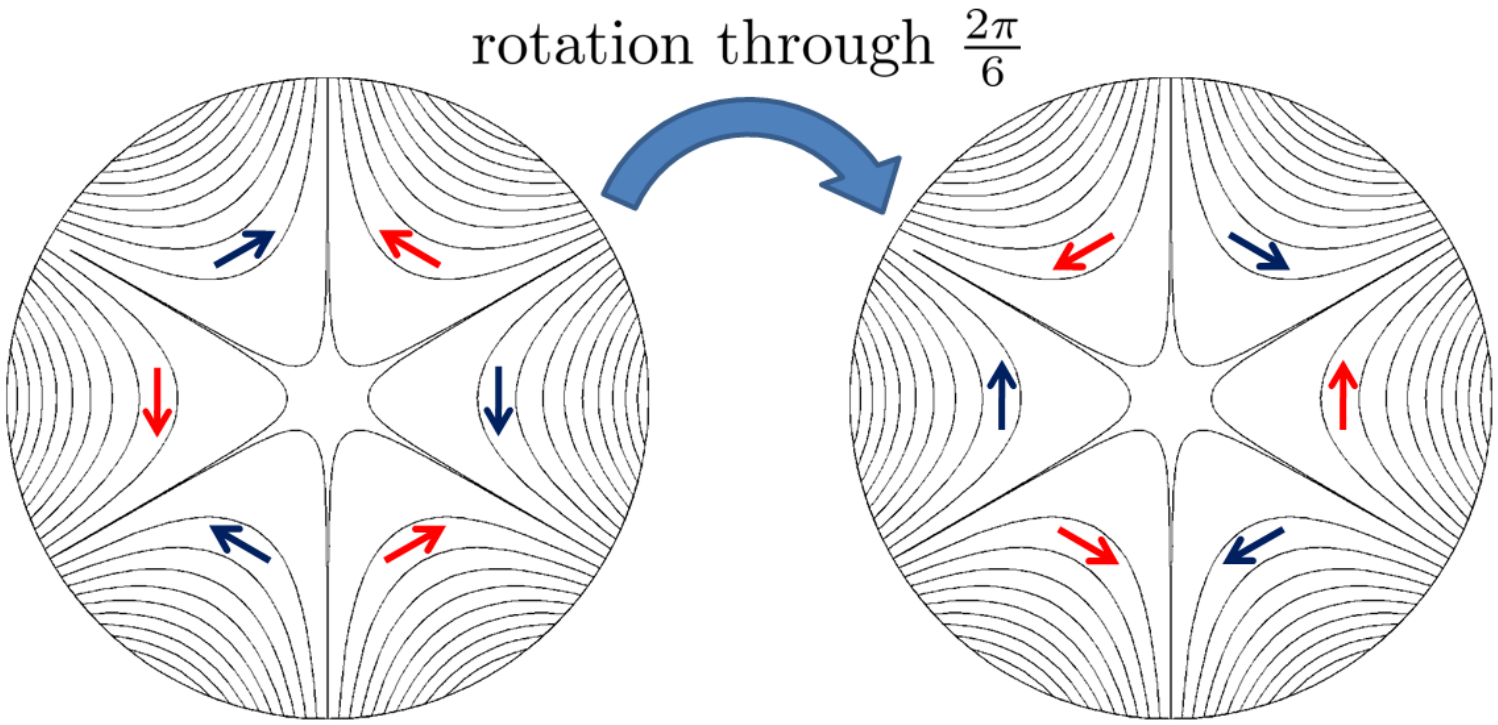

Since this symmetry is imposed by the geometry of the magnet, any multipole field within the magnet must obey this symmetry. This restricts the multipole components that may be present, at least in the design.

Consider a field given by:

$$B_y + iB_x = |C_n|e^{-in\theta_n}r^{n-1}e^{i(n-1)\theta} + |C_m|e^{-im\theta_m}r^{m-1}e^{i(m-1)\theta}. \tag{11}$$

If the geometry of the magnet is such that the field simply changes sign under a rotation through π/n, then the "extra" harmonic must satisfy:

$$e^{-i\pi\frac{m}{n}} = -1, \tag{12}$$

therefore:

$$\frac{m}{n} = 1,\ 3,\ 5,\ 7\ \ldots \tag{13}$$

We see that only *higher* harmonics are allowed; and the indices of the higher harmonics must be an odd integer multiple of the main harmonic.

Allowed and forbidden harmonics

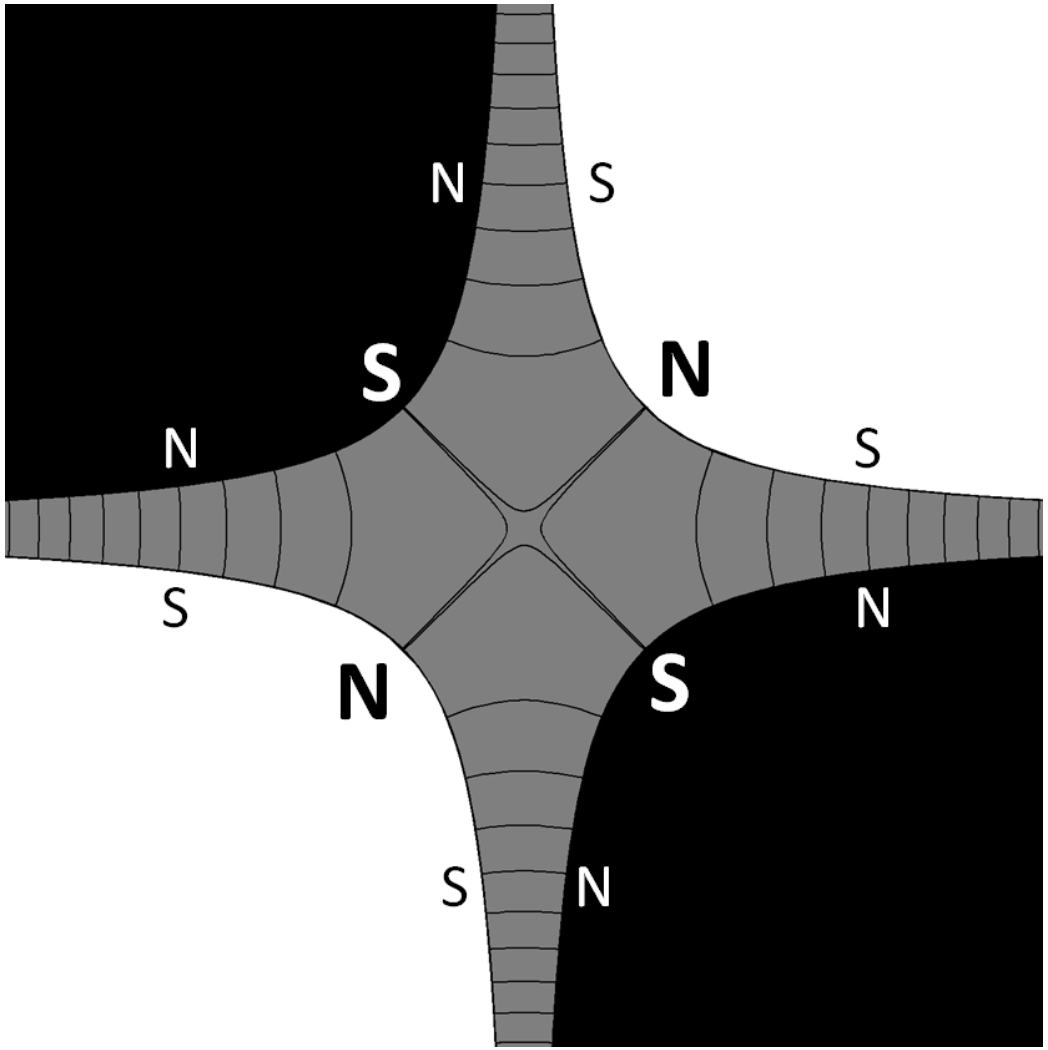

For a dipole, $n = 1$, so the allowed harmonics are $m = 3, 5, 7 \ldots$
For a quadrupole, $n = 2$, and the allowed harmonics are
$m = 6, 10, 14 \ldots$

Of course, this argument cannot tell us the strengths of the allowed harmonics: those depend on the details of the design.

It is also a fact that a magnet, when fabricated, will never exhibit perfectly the symmetry with which it was designed. Therefore, a real physical magnet will generally include *all* harmonics to some extent, not just the harmonics allowed by the ideal symmetry.

However, for a carefully fabricated magnet, the harmonics forbidden by the ideal symmetry should be small in comparison to the allowed harmonics; and it should be possible to predict the sizes of the allowed harmonics accurately from the design.

Knowing the multipole components of magnets in an accelerator is important for understanding the beam dynamics.

Construction tolerances will mean that the strengths of the multipoles present in the magnet will differ from those in the design.

This leads us to consider how to determine the multipole components from measurements of the magnetic field.

There are many possible approaches to the problem: we shall consider two, for illustration, and only go as far as necessary to understand some of the pros and cons.

The field may be represented as:

$$B_y + iB_x = \sum_n C_n (x + iy)^{n-1}, \tag{14}$$

where the real parts of the coefficients C_n give the normal multipole strengths, and the imaginary parts give the skew multipole strengths.

If we take a set of measurements of B_y and B_x along the x axis, then $y = 0$ at each measurement point, and the normal multipoles can be found by fitting a polynomial to B_y *vs* x, and the skew multipoles can be found by fitting a polynomial to B_x *vs* x.

Let us see how this works with some invented data...

We construct a quadruople field with higher harmonics 3, 4 and 5, and fit a quartic to the field "data":

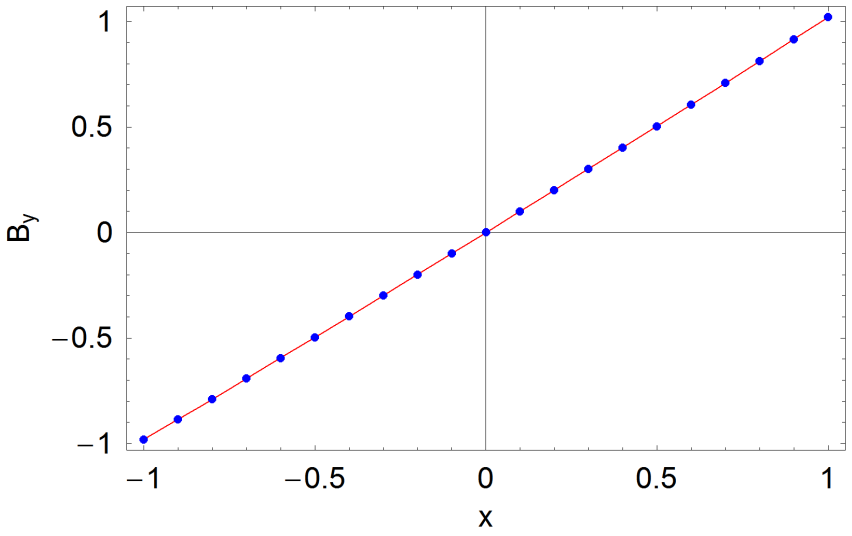

n	actual value	fitted value
2	1.000	1.000
3	0.010	0.010
4	0.001	0.001
5	0.010	0.010

So far so good. But what happens if we include a higher-order multipole that we do not fit?

Now we add a higher harmonic $n = 6$, but still fit the field data with a quartic:

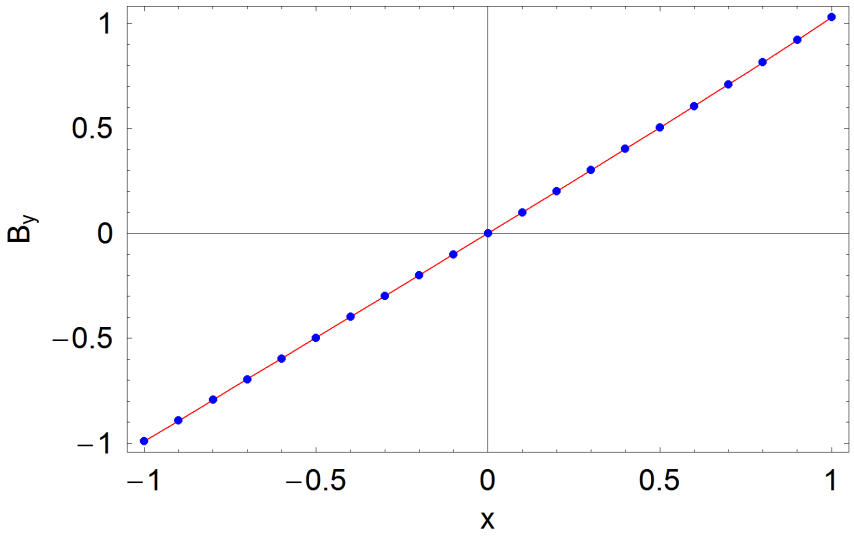

n	actual value	fitted value
2	1.0000	0.9972
3	0.0100	0.0100
4	0.0010	0.0131
5	0.0100	0.0100
6	0.0100	-

We now have significant errors on the $n = 2$ and $n = 4$ multipole field strengths.

The reason for the discrepancy perhaps starts to become clear if we plot the deviation from the "nominal" quadrupole field.

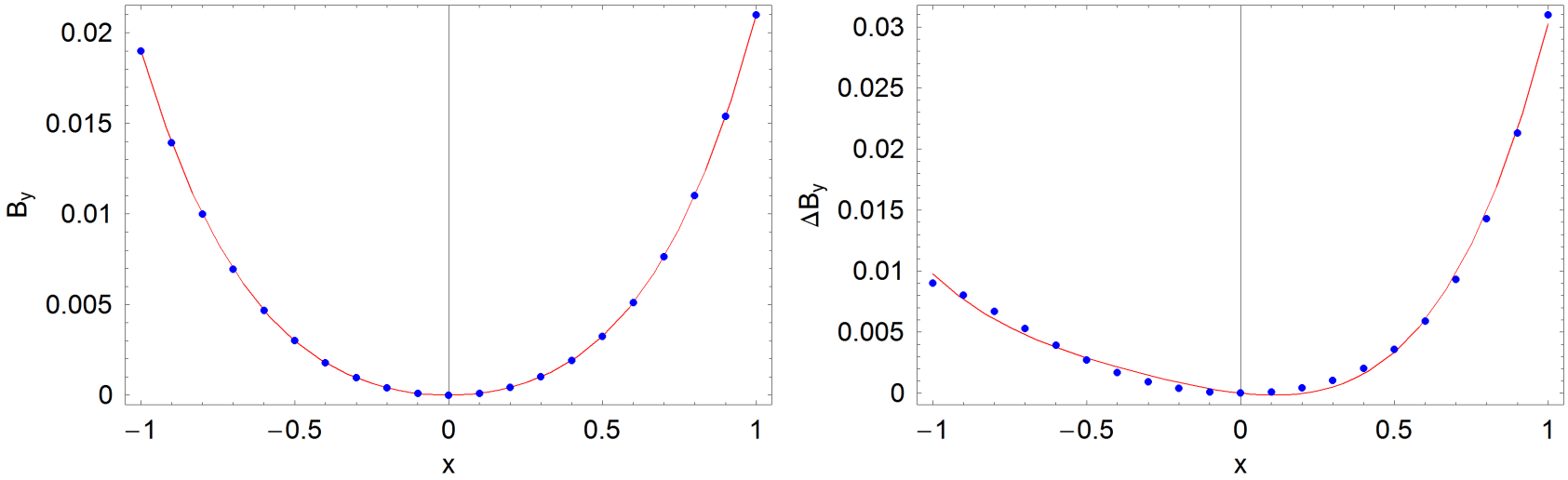

With only components present up to $n = 5$ (left hand plot), the fit is essentially perfect. But with a higher component ($n = 6$, right hand plot) that we do not fit, there are significant residuals.

The real problem is that mathematically, the basis functions that we use to fit the data (monomials in x and, possibly, y) are not orthogonal. This means that data constructed from one monomial can be fitted, with non-zero strength, with a completely different monomial.

Although this does not invalidate the technique altogether, it does make it a little difficult to apply accurately. Ideally, we need to know in advance which multipole components are present.

However, there is a more robust technique...

Instead of expressing the field in Cartesian coordinates, let us write the same field in polar coordinates:

$$B_y + iB_x = \sum_n C_n r^{n-1} e^{i(n-1)\theta}. \tag{15}$$

Now suppose that we take a set of measurements of B_y and B_x at fixed $r = r_0$, but at M equally spaced steps in $\theta = 2\pi m/M$, where $m = 1 \ldots M$.

We then notice that:

$$\begin{aligned} \sum_{m=1}^{M} (B_y + iB_x)_m e^{-2\pi i(n'-1)\frac{m}{M}} &= \sum_{m=1}^{M} \sum_n C_n r_0^{n-1} e^{2\pi i(n-n')\frac{m}{M}} \\ &= M C_{n'} r_0^{n'-1}. \end{aligned} \tag{16}$$

Hence:

$$C_n = \frac{1}{M r_0^{n-1}} \sum_{m=1}^{M} (B_y + iB_x)_m e^{-2\pi i(n-1)\frac{m}{M}}. \tag{17}$$

The advantage of using polar coordinates, over Cartesian coordinates, is that the basis functions, $e^{i(n-1)\theta}$, are orthogonal. Mathematically, we have:

$$\sum_{m=1}^{M} e^{2\pi i(n-1)\frac{m}{M}} e^{-2\pi i(n'-1)\frac{m}{M}} = \begin{cases} 0 & \text{if} \quad n \neq n' \\ \\ M & \text{if} \quad n = n' \end{cases} \tag{18}$$

The orthogonality means that the value we determine for one multipole component is completely unaffected by the presence of other multipole components.

Determining the multipole coefficients C_n amounts to carrying out a discrete Fourier transform on the field data measured on a cylinder inscribed through the magnet.

A further advantage of the polar basis comes from the fact that the radius of the cylinder on which the field data are collected appears as $1/r_0^{n-1}$ in the expression for the coefficients C_n, equation (17).

Suppose that there is some error in the field measurements. This will lead to some error in the values of C_n that we determine. If we reconstruct the field (e.g. for particle tracking), then there will be some error in the calculated field. However, this error will decrease as r^{n-1}, as we go towards the centre of the magnet (where the beam is).

Of course, if we try to extrapolate the field outside the cylinder of radius r_0, then any errors will *increase* as some power of the distance from the centre.

There are some important advantages to describing a field in terms of a mode decomposition, instead of a set of numerical field values on a grid:

- A description of the field in terms of mode coefficients is very much more compact than a description in terms of numerical field data.
- A field constructed from mode coefficients is guaranteed to satisfy Maxwell's equations: numerical field data are not.
- Measurement noise can be "smoothed" by suppressing higher-order modes.
- Errors can be represented in a realistic way by introducing higher-order modes.
- A number of beam dynamics analysis tools require mode decompositions.

The polar basis for fitting multipole field components generalises nicely to three-dimensional fields. But, since we have not so far discussed such fields at all, before showing how the field fitting works, we need to discuss solutions to Maxwell's equations for three-dimensional magnets.

As before, the relevant equations are:

$$\nabla \cdot \vec{B} = 0, \quad \text{and} \quad \nabla \times \vec{B} = 0. \tag{19}$$

Any field that satisfies these equations is a possible magnetic field in free space. So far, we have considered only multipole fields, that are independent of one coordinate; but this is not very realistic.

A field that satisfies Maxwell's equations (19) is given by:

$$B_x = -B_0 \frac{k_x}{k_y} \sin k_x x \sinh k_y y \sin k_z z, \quad (20)$$

$$B_y = B_0 \cos k_x x \cosh k_y y \sin k_z z, \quad (21)$$

$$B_z = B_0 \frac{k_z}{k_y} \cos k_x x \sinh k_y y \cos k_z z, \quad (22)$$

where:

$$k_y^2 = k_x^2 + k_z^2. \quad (23)$$

There are a number of variations on this field, for example, with the hyperbolic function appearing in the x or z coordinates; or, with different phases in x and/or z. However, the above representation is particularly convenient for describing insertion devices (wigglers and undulators), as we shall now discuss.

$$
\begin{aligned}
B_x &= -B_0 \frac{k_x}{k_y} \sin k_x x \, \sinh k_y y \, \sin k_z z, \\
B_y &= B_0 \cos k_x x \, \cosh k_y y \, \sin k_z z, \\
B_z &= B_0 \frac{k_z}{k_y} \cos k_x x \, \sinh k_y y \, \cos k_z z,
\end{aligned}
$$

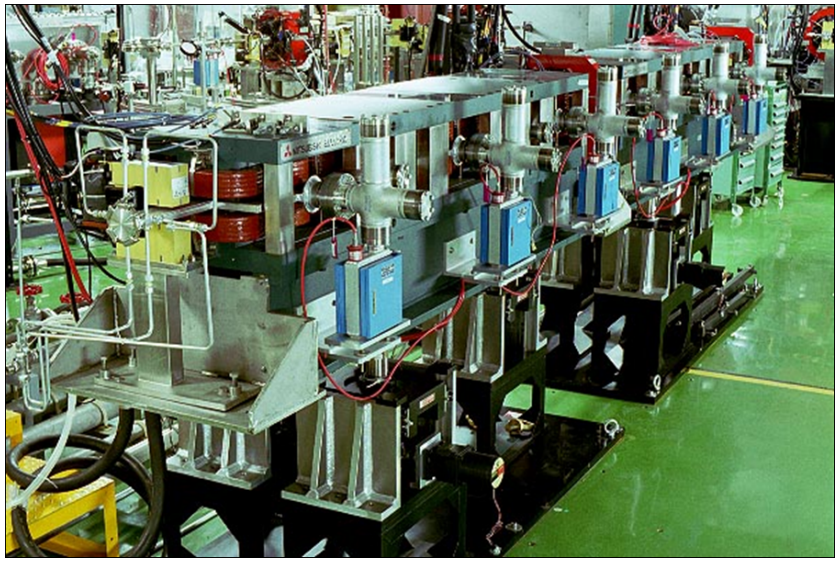

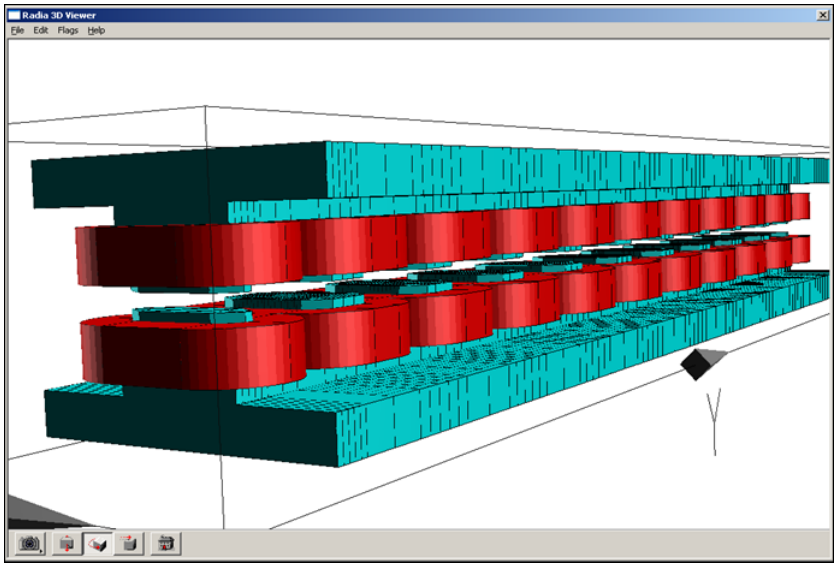

Normal-conducting electromagnetic wiggler at the KEK Accelerator Test Facility.

If we take $k_x = 0$, then the field becomes:

$$B_x = 0, \tag{24}$$
$$B_y = B_0 \cosh k_z y \sin k_z z, \tag{25}$$
$$B_z = B_0 \sinh k_z y \cos k_z z. \tag{26}$$

The above equations describe a field that varies sinusoidally in z, and has no horizontal (x) component at all. This is a field that could only occur in an insertion device with infinite length, and infinite width.

A better description would take account of the fact that the longitudinal variation of the field will not be perfectly sinusoidal. We can account for this by superposing fields with different values of k_z:

$$B_x = 0, \tag{27}$$

$$B_y = \int \tilde{B}(k_z) \cosh k_z y \sin k_z z \, dk_z, \tag{28}$$

$$B_z = \int \tilde{B}(k_z) \sinh k_z y \cos k_z z \, dk_z. \tag{29}$$

We see that if we take measurements of B_y as a function of z in the plane $y = y_0$ (for fixed y_0), then we can obtain the *mode coefficients* $\tilde{B}(k_z)$ by a (discrete) Fourier transform.

This allows us to reconstruct all field components, at all locations within the field.

Suppose we measure B_y at a set of locations $z = z_\ell$, where:

$$z_\ell = \frac{\ell}{N} z_{\text{max}}, \qquad \ell = -N, -N+1, -N+2, \ldots, N. \tag{30}$$

N is an integer, and the field has effectively fallen to zero at $z = \pm z_{\text{max}}$.

We obtain the mode coefficients from:

$$\tilde{B}_n = \frac{1}{2N \cosh(n k_z y_0)} \sum_{\ell=-N}^{N} B_y(z_\ell) \sin\left(n k_z z_\ell\right), \tag{31}$$

where $k_z = \pi / z_{\text{max}}$.

And the field at any point can be reconstructed from:

$$B_y(y,z) = \sum_{n=-N}^{N} \tilde{B}_n \cosh\left(n k_z y\right) \sin\left(n k_z z\right), \tag{32}$$

$$B_z(y,z) = \sum_{n=-N}^{N} \tilde{B}_n \sinh\left(n k_z y\right) \cos\left(n k_z z\right). \tag{33}$$

Let us see what happens in a simple example – again, using "invented" data. The left hand plot shows the field data (points), and the reconstructed field (red line). The right hand plot shows the mode coefficients, from which the reconstruction is obtained. Measurements are made along $y = 0.25$.

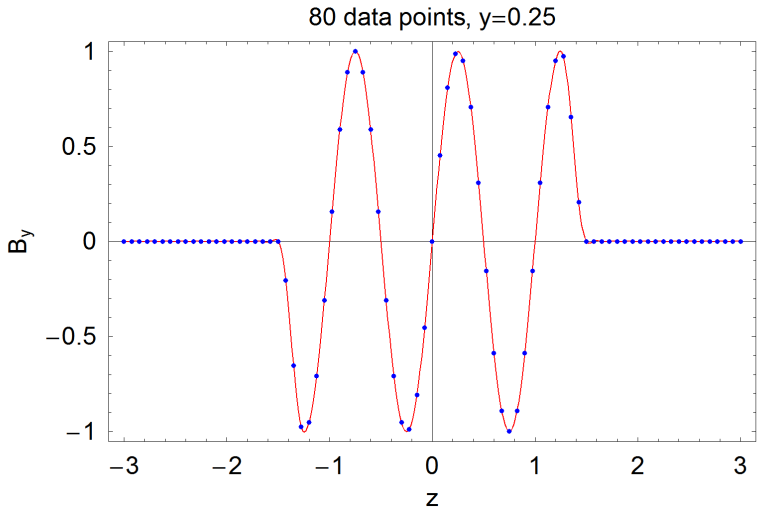

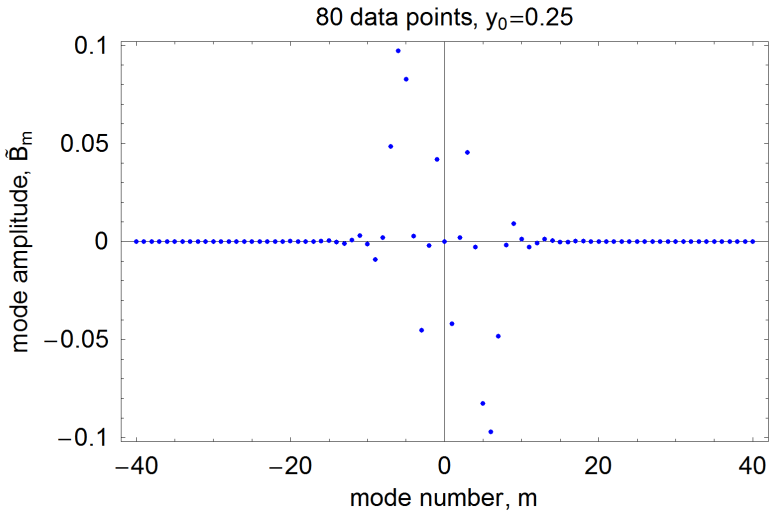

Mathematically, the reconstructed field must fit the data exactly. However, the interpolation between the data points is only reliable if the mode coefficients are small for large mode number.

If the data are too sparse, then we can determine only a small number of modes. The previous plots were constructed from 80 measurement points. What happens if we reduce the number of measurement points to 30?

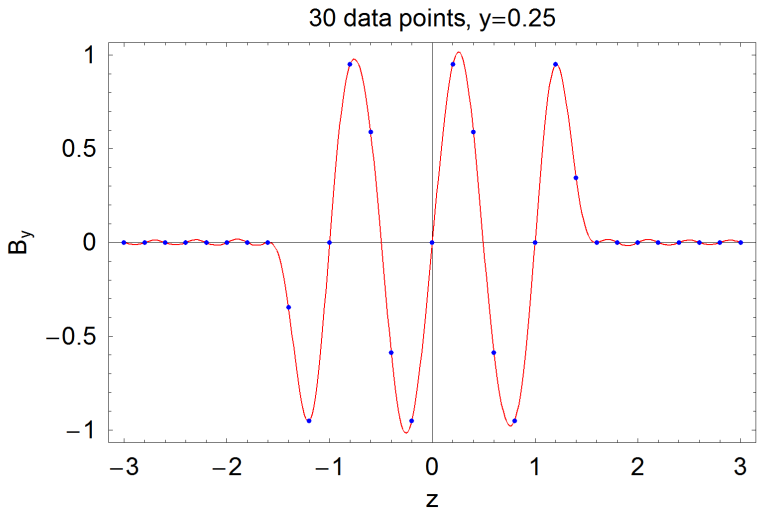

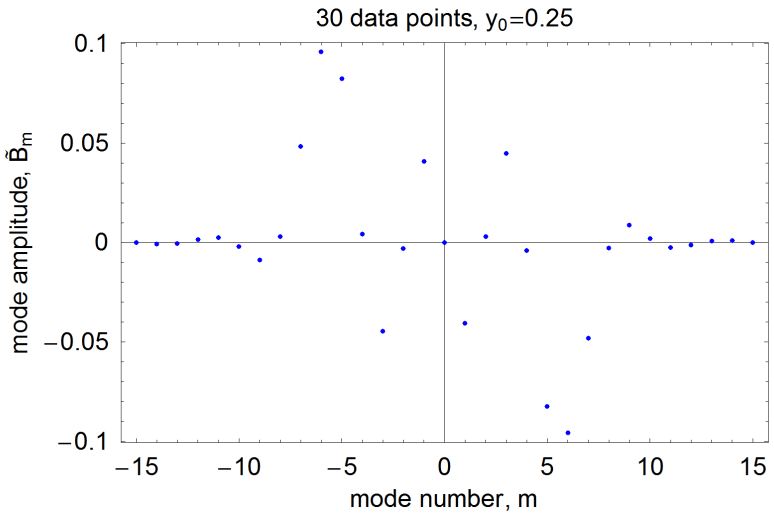

The data are still fitted exactly, but there is significant "wiggle" between the data points, where the field is really close to zero.

Using our mode coefficients, we can reconstruct the field along the z axis:

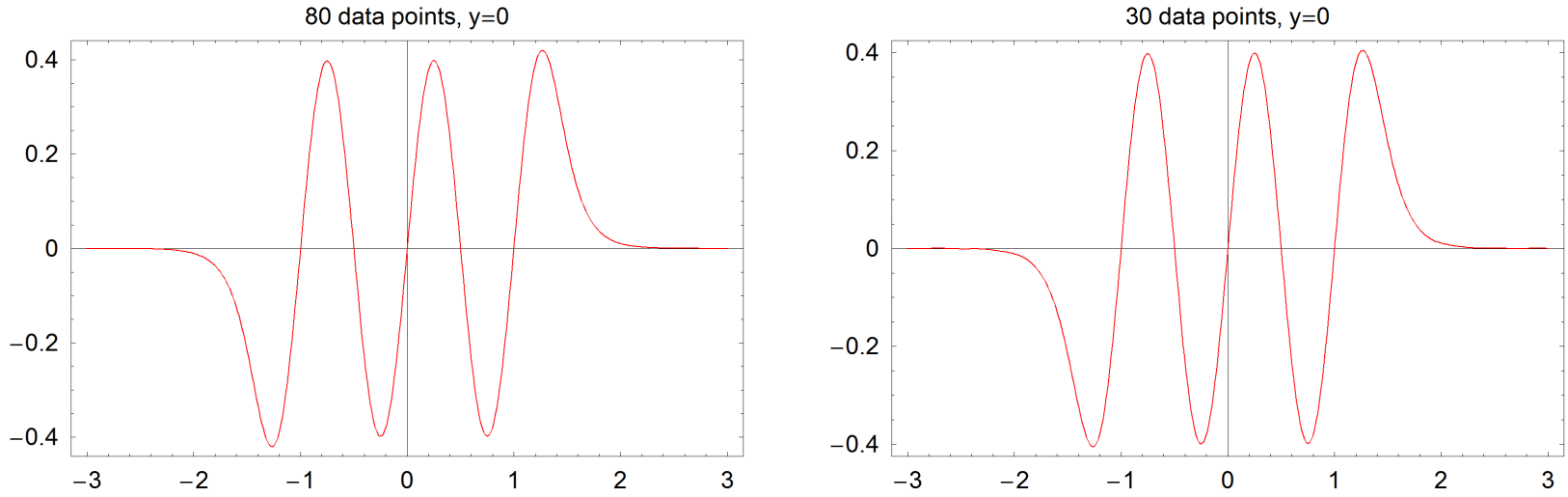

Note that the field extends out further in z: the fringe field increases as we approach the mid-plane. Also note that the "wiggles" beyond the fringe field have been smoothed out: this is a result of the hyperbolic dependence of the field on y. If we had fitted the data on $y = 0$, the residuals would have *increased* exponentially with increasing y.

If we look at the field variation with vertical position (y), we see that the field variation is not sensitive to the number of modes:

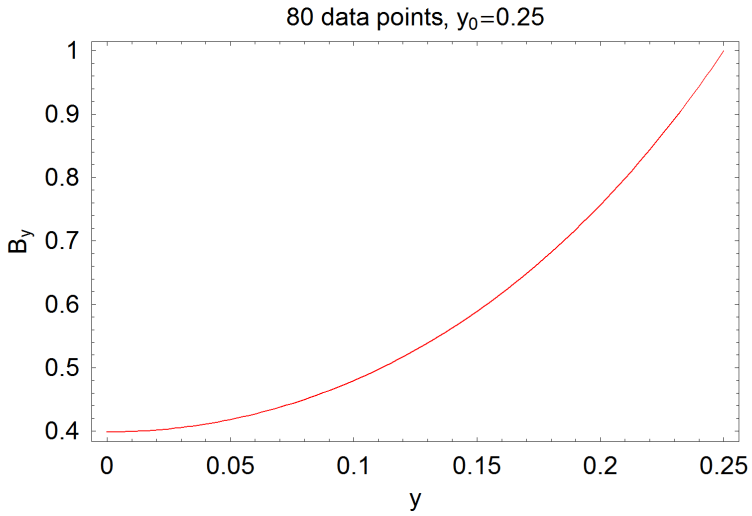

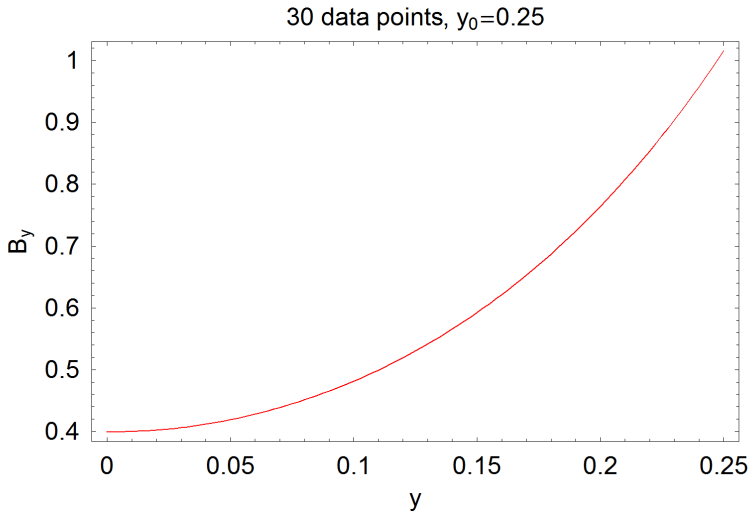

Again, this is a result of the hyperbolic dependence of the field on the vertical coordinate.

However, if we try to extrapolate to $y > y_0$, where $y = y_0$ is the line of the fit, then unpredictable behaviour can result...

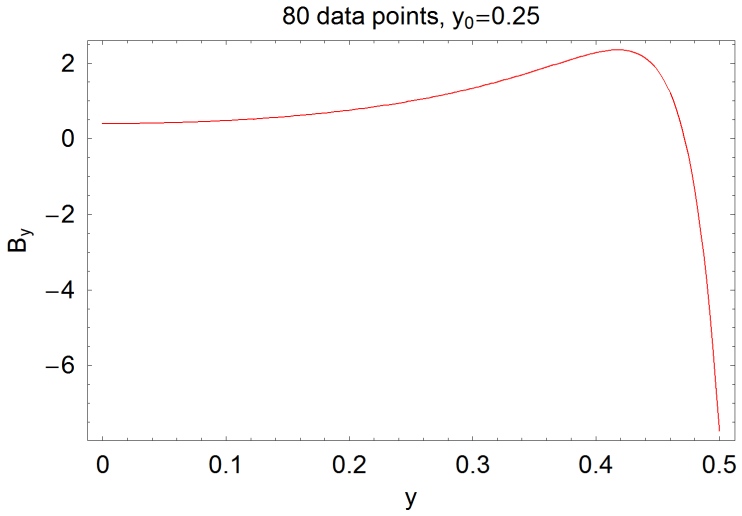

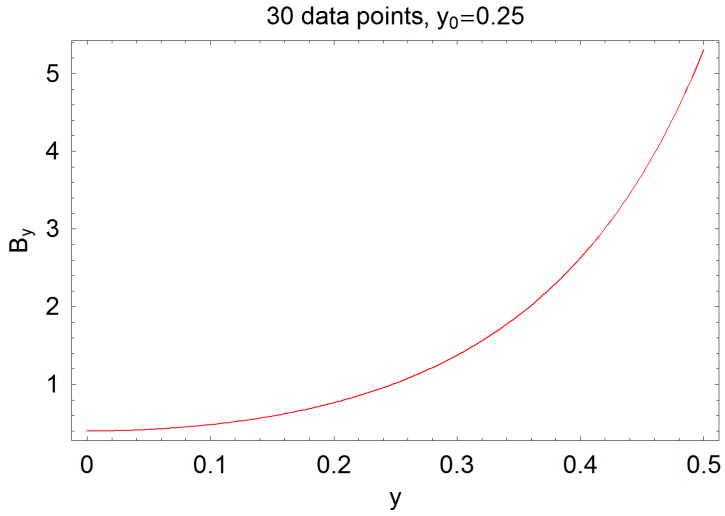

Of course, the above example still describes a field that is independent of one of the coordinates. However, generalisation to include a dependence on x is straightforward.

Generally, from (21), we can write the vertical field component as:

$$B_y = \sum_m \tilde{B}_{mn} \cos mk_x x \cosh k_y y \sin nk_z z, \tag{34}$$

where:

$$k_y^2 = m^2 k_x^2 + n^2 k_z^2. \tag{35}$$

The mode coefficients $\tilde{B}_{mn}$ (note the double index) can be obtained from a 2D discrete Fourier transform on a plane of fixed y. As in the example, it is beneficial to choose the plane $y = y_0$ so that the planes $y = \pm y_0$ bound the region of interest. Outside this region, the fields will diverge.

Another issue with this choice of basis functions is the value of the horizontal parameter $k_x = \pi/x_{\mathsf{max}}$.

Ideally, one will make measurements over a sufficiently wide region that the field drops to zero at $x = \pm x_{\mathsf{max}}$.

This may be possible in principle for some simple wigglers and undulators, but may not always be practicable, even in these cases.

An alternative approach, and one that is preferable in many situations, is to use a cylindrical basis for the mode decomposition.

In cylindrical polar coordinates, a field satisfying Maxwell's equations can be represented by:

$$B_\rho = \int dk_z \sum_m \tilde{B}_m(k_z) I'_m(k_z\rho) \sin m\theta \cos k_z z, \quad (36)$$

$$B_\theta = \int dk_z \sum_m \tilde{B}_m(k_z) \frac{m}{k_z\rho} I_m(k_z\rho) \cos m\theta \cos k_z z, \quad (37)$$

$$B_z = -\int dk_z \sum_m \tilde{B}_m(k_z) I_m(k_z\rho) \sin m\theta \sin k_z z. \quad (38)$$

Here, the functions $I_m(r)$ are modified Bessel functions: broadly speaking, they are to regular Bessel functions as hyperbolic trigonometric functions are to regular trigonometric functions.

The mode coefficients $\tilde{B}_m(k_z)$ may be obtained, for example, by a 2D discrete Fourier transform of the radial field component B_ρ on the surface of a cylinder.

We can draw a direct connection between the 3D polar basis, and the multipole decomposition in 2D. We use the fact that the modified Bessel functions have an expansion (for small ξ):

$$I_m(\xi) = \frac{\xi^m}{2^m \Gamma(1+m)} + O(m+1). \tag{39}$$

Therefore, if the mode coefficients are given by:

$$\tilde{B}_m(k_z) = 2^m \Gamma(1+m) C_m \frac{\delta(k_z)}{m k_z^{m-1}}, \tag{40}$$

where $\delta()$ is the Dirac delta function, then:

$$B_\rho = \sum_m C_m \rho^{m-1} \sin m\theta, \tag{41}$$

$$B_\theta = \sum_m C_m \rho^{m-1} \cos m\theta, \tag{42}$$

$$B_z = 0. \tag{43}$$

Then, we note that:

$$B_x = B_\rho \cos\theta - B_\theta \sin\theta, \tag{44}$$
$$B_y = B_\rho \sin\theta + B_\theta \cos\theta, \tag{45}$$

to find:

$$B_x = \sum_m C_m \rho^{m-1} \sin(m-1)\theta, \tag{46}$$
$$B_y = \sum_m C_m \rho^{m-1} \cos(m-1)\theta. \tag{47}$$

Hence:

$$B_y + iB_x = \sum_m C_m (x+iy)^{m-1}. \tag{48}$$

This is the familiar form for a multipole field. Since the original coefficients $\tilde{B}_m$ are real, it follows from (40) that the coefficients C_m are also real, so equations (36)-(38) represent a 3D normal multipole. A skew multipole is just obtained by a rotation through θ by $\pi/2$.

The connection between the 3D mode decomposition in the cylindrical basis and the usual representation of a multipole field gives us a nice interpretation of the mode coefficients $\tilde{B}_m$.

The coefficient $\tilde{B}_m(k_z)$ is essentially the longitudinal Fourier amplitude of the $2m$-pole field in the magnet. We should remember, of course, that multipole fields only really exist in infinitely long, uniform magnets. The representation (36)-(38), however, can be used to describe realistic, 3D fields.

We mentioned above that the mode coefficients $\tilde{B}_m(k_z)$ may be obtained by a 2D discrete Fourier transform of the radial field component B_ρ on the surface of a cylinder.

As usual, it is beneficial to choose the radius of this cylinder to be as large as possible: inside the cylinder, errors in the fit decrease exponentially; outside the cylinder, the errors increase exponentially.

With good field data, it is possible to achieve a very good fit. As an example, the following slides show fits to a model for a permanent magnet wiggler for the TESLA damping ring. The (nominal, on-axis) peak field is 1.7 T, and the wiggler period is 0.4 m. The fits were obtained using 18 azimuthal and 100 longitudinal modes, on a cylinder of radius 9 mm.

Field fit to TESLA damping wiggler

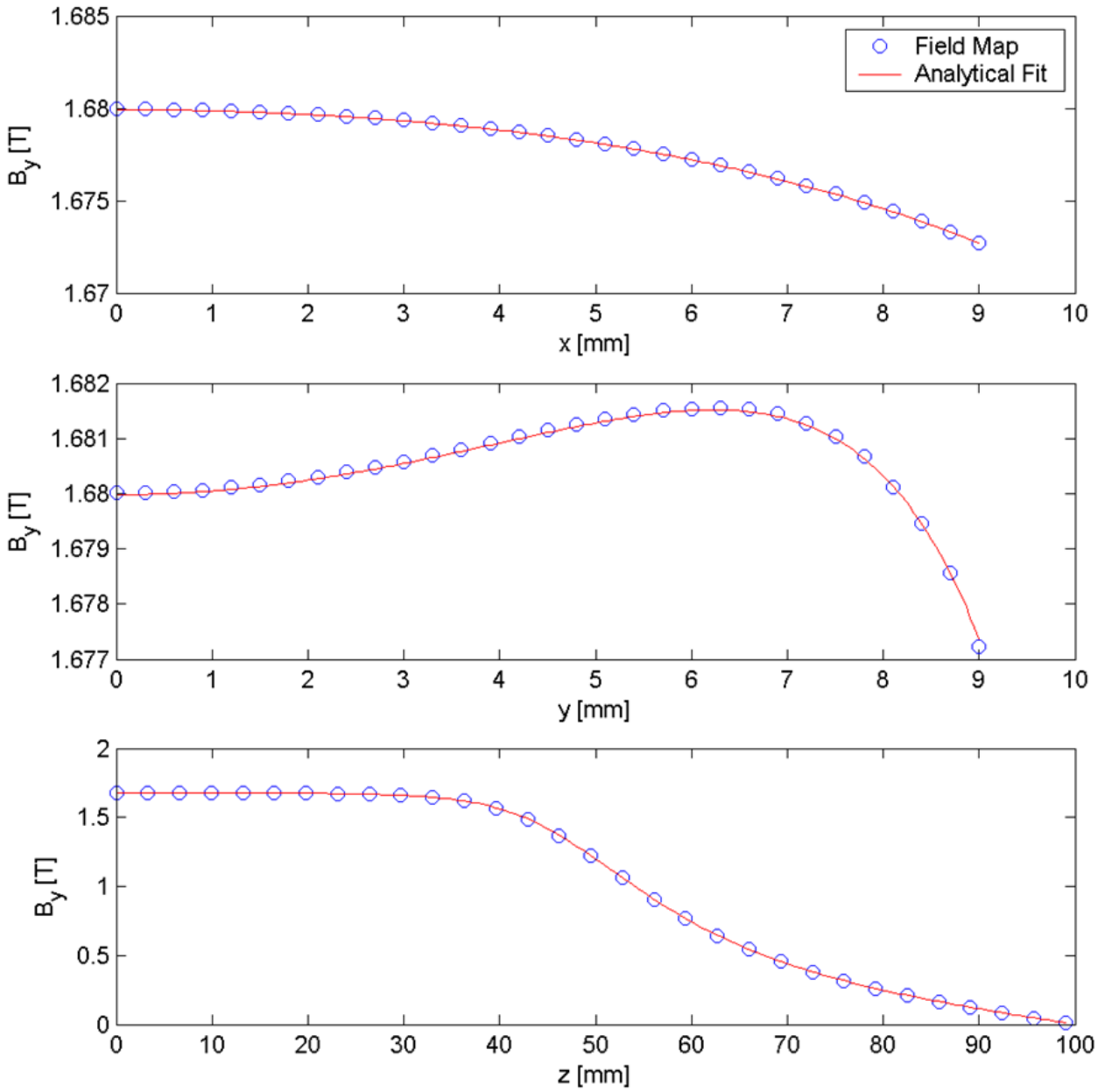

Field fit to TESLA damping wiggler: residuals

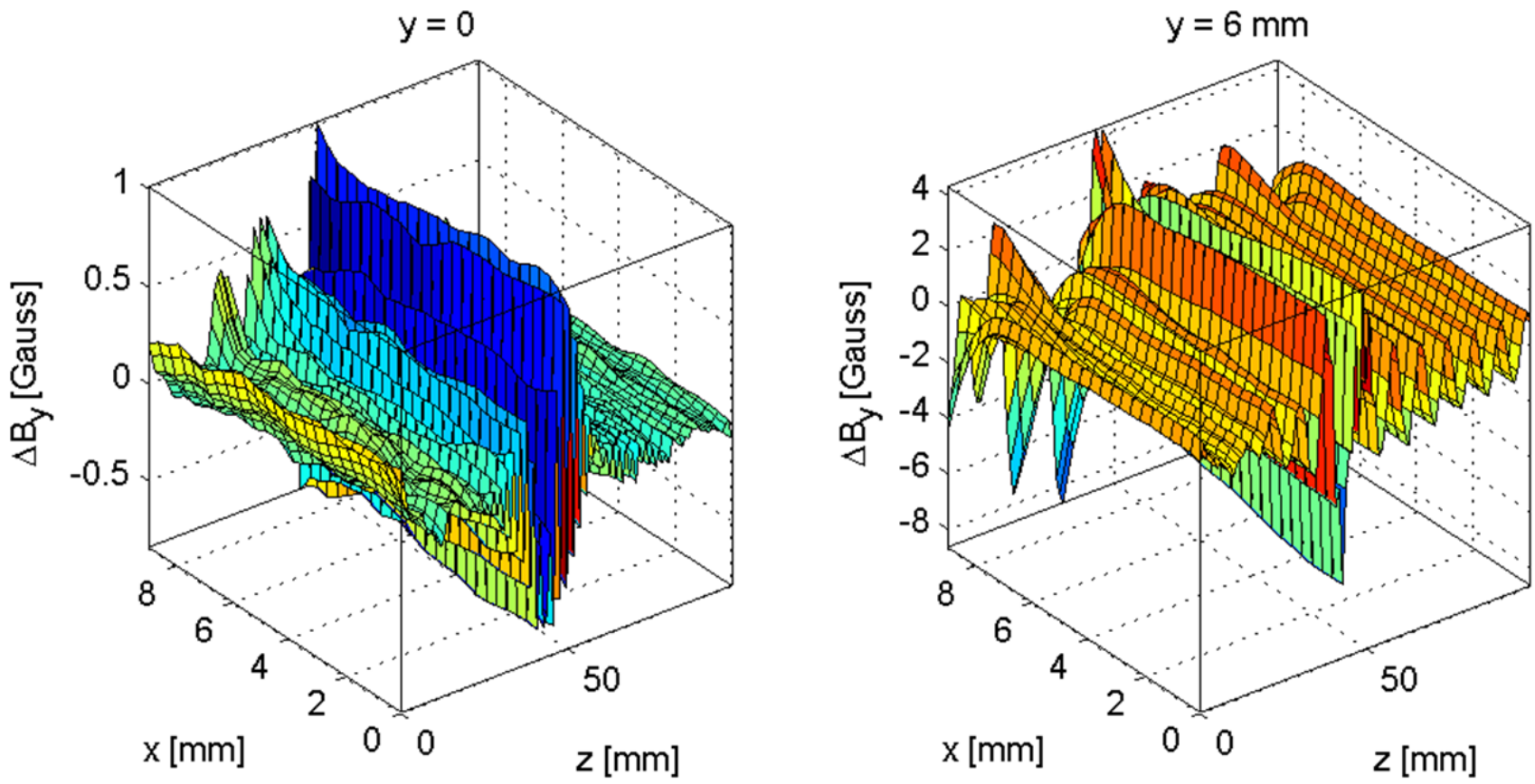

Often, the apertures in accelerator magnet (particularly, in insertion devices) are not circular: the horizontal aperture is wider than the vertical. In such cases, a good fit can be obtained over a wider region by using an elliptical cross-section for the cylinder, rather than a circular cross-section.

It is possible to perform an inverse Fourier transform on the mode coefficients in the longitudinal dimension z, while retaining the mode decomposition in θ. Then, we obtain a representation in which the "multipole component" appears as a function of z. This approach leads to the idea of *generalised gradients*.

For further information on both these topics, see the book by Alex Dragt:

"Lie methods for nonlinear dynamics with applications to accelerator physics."
http://www.physics.umd.edu/dsat/dsatliemethods.html

Summary of Lecture 1

Maxwell's equations impose strong constraints on magnetic fields that may exist.

The linearity of Maxwell's equations means that complicated fields may be expressed as a superposition of simpler fields.

In two dimensions, it is convenient to represent fields as a superposition of multipole fields.

Multipole fields may be generated by sinusoidal current distributions on a cylinder bounding the region of interest.

In regions without electric currents, the magnetic field may be derived as the gradient of a scalar potential.

The scalar potential is constant on the surface of a material with infinite permeability. This property is useful for defining the shapes of iron poles in multipole magnets.

Summary of Lecture 2

Symmetries in multipole magnets restrict the multipole components that can be present in the field.

It is useful to be able to find the multipole components in a given field from numerical field data: but this must be done carefully, if the results are to be accurate.

Usually, it is advisable to calculate multipole components using field data on a surface enclosing the region of interest: any errors or residuals will decrease exponentially within that region, away from the boundary. Outside the boundary, residuals will increase exponentially.

Techniques for finding multipole components in two dimensional fields can be generalised to three dimensions, allowing analysis of fringe fields and insertion devices.

In two or three dimensions, it is possible to use a Cartesian basis for the field modes; but a polar basis is sometimes more convenient.

In lecture 1, we used a scalar potential for the magnetic field to derive the shape for the pole face of a multipole magnet.

The scalar potential Φ is defined such that:

$$\vec{B} = -\nabla\Phi. \tag{49}$$

With this definition, the equation $\nabla \times \vec{B} = 0$ is automatically satisfied. The equation $\nabla \cdot \vec{B} = 0$ leads to Laplace's equation for the scalar potential:

$$\nabla^2\Phi = 0. \tag{50}$$

However, the scalar potential is only defined in the absence of currents. More generally, we need to use a vector potential $\vec{A}$. In fact, in the most general case of time-dependent electric and magnetic fields, we need both a scalar potential ϕ, and a vector potential $\vec{A}$:

$$\vec{B} = \nabla \times \vec{A}, \quad \text{and} \quad \vec{E} = -\nabla\phi - \frac{\partial \vec{A}}{\partial t}. \tag{51}$$

Some important methods for beam dynamics analysis use the potentials ϕ and $\vec{A}$, rather than the fields. It is therefore useful to have expressions for the potentials corresponding to the expressions for the fields we have derived in the main part of these lectures.

For the case of interest here (a magnetostatic field, and zero electric field), we can assume that ϕ is independent of position, and $\vec{A}$ is independent of time.

If we allow the presence of nonmagnetic materials ($\mu = \mu_0$) carrying an electric current density $\vec{J}$, then substituting from (51) into Maxwell's equations gives:

$$\nabla \cdot \vec{B} = \nabla \cdot \nabla \times \vec{A} \equiv 0, \tag{52}$$

and:

$$\nabla \times \vec{B} = \nabla \times \nabla \times \vec{A} \equiv \nabla(\nabla \cdot \vec{A}) - \nabla^2 \vec{A} = \mu_0 \vec{J}. \tag{53}$$

Maxwell's equation $\nabla \cdot \vec{B} = 0$ is automatically satisfied by any vector potential $\vec{A}$, by virtue of a vector identity (the divergence of the curl of any vector field is zero).

Maxwell's equation $\nabla \times \vec{H} = \vec{J}$ (assuming static fields) is satisfied, if the vector potential $\vec{A}$ satisfies:

$$\nabla^2 \vec{A} - \nabla(\nabla \cdot \vec{A}) = -\mu_0 \vec{J}. \tag{54}$$

Now, we observe that since $\vec{B} = \nabla \times \vec{A}$, and $\nabla \times \nabla\psi$ is identically zero for any scalar field ψ, we can define a new potential $\vec{A}' = \vec{A} + \nabla\psi$ that gives exactly the same field as $\vec{A}$. We can use this property of the fields and potentials, known as *gauge invariance*, to simplify equation (54).

Suppose that we have a vector potential $\vec{A}$ for which:

$$\nabla \cdot \vec{A} = f, \tag{55}$$

where f is some function of position. Then, if we define:

$$\vec{A}' = \vec{A} + \nabla\psi, \tag{56}$$

where ψ satisfies Poisson's equation:

$$\nabla^2\psi = -f, \tag{57}$$

then $\vec{A}'$ gives the same field $\vec{B}$ as $\vec{A}$, and:

$$\nabla \cdot \vec{A}' = \nabla \cdot \vec{A} + \nabla^2\psi = 0. \tag{58}$$

In other words, if we can solve Poisson's equation (57) for ψ, then we can make a *gauge transformation* to a vector potential that has vanishing divergence.

Let us suppose that we find a vector potential that has vanishing divergence:

$$\nabla \cdot \vec{A} = 0. \tag{59}$$

Equation (59) amounts to a condition that specifies a particular choice of gauge: this particular choice (i.e. with zero divergence) is known as the Coulomb gauge. It is useful, because equation (54) for the vector potential then takes the simpler form:

$$\nabla^2 \vec{A} = -\mu_0 \vec{J}. \tag{60}$$

This is Poisson's equation, which has the standard solution:

$$\vec{A}(\vec{r}) = -\frac{\mu_0}{4\pi} \int \frac{\vec{J}(\vec{r}\,')}{|\vec{r} - \vec{r}\,'|} \, d^3 r'. \tag{61}$$

Now, consider the potential given by:

$$A_x = 0, \quad A_y = 0, \quad A_z = -\mathrm{Re}\,\frac{C_n(x+iy)^n}{n}. \tag{62}$$

Taking derivatives, we find that:

$$\frac{\partial A_z}{\partial x} = -\mathrm{Re}\,C_n(x+iy)^{n-1}, \quad \text{and} \quad \frac{\partial A_z}{\partial y} = \mathrm{Im}\,C_n(x+iy)^{n-1}. \tag{63}$$

Hence:

$$\begin{aligned} \vec{B} &= \nabla \times \vec{A}, \\ &= \left(\frac{\partial A_z}{\partial y}, -\frac{\partial A_z}{\partial x}, 0\right), \\ &= \left(\mathrm{Im}\,C_n(x+iy)^{n-1}, \mathrm{Re}\,C_n(x+iy)^{n-1}, 0\right). \end{aligned} \tag{64}$$

Therefore, we have:

$$B_y + iB_x = C_n(x + iy)^{n-1},$$

which is just the multipole field (1).

We have shown that the potential:

$$A_x = 0, \quad A_y = 0, \quad A_z = -B_{\text{ref}} \sum_{n=1}^{\infty} (b_n + ia_n) \frac{\text{Re}(x + iy)^n}{nR_{\text{ref}}^{n-1}}, \quad (65)$$

gives the multipole field (1):

$$B_y + iB_x = B_{\text{ref}} \sum_{n=1}^{\infty} (b_n + ia_n) \left(\frac{x + iy}{R_{\text{ref}}} \right)^{n-1}.$$

Note also that:

$$\nabla \cdot \vec{A} = \frac{\partial A_x}{\partial x} + \frac{\partial A_y}{\partial y} + \frac{\partial A_z}{\partial z} = 0, \quad (66)$$

so this potential satisfies the Coulomb gauge condition.

Note that the longitudinal field component derived from the multipole potential (65) is:

$$B_z = \frac{\partial A_y}{\partial x} - \frac{\partial A_x}{\partial y} = 0. \tag{67}$$

In order to generate a solenoidal field, with $B_z = \text{constant} \neq 0$, we need to introduce non-zero components in A_x, A_y, or both. For example:

$$A_x = -\frac{1}{2} B_{\text{sol}} y, \quad A_y = \frac{1}{2} B_{\text{sol}} x. \tag{68}$$

While it is convenient, for beam dynamics, to work in a gauge with only the z component of the vector potential non-zero, this is not possible for solenoidal fields.

Finally, we give the vector potentials corresponding to 3D fields. In the Cartesian basis (20)-(22):

$$\begin{aligned} B_x &= -\tilde{B}(k_x, k_z)\frac{k_x}{k_y}\sin k_x x \sinh k_y y \sin k_z z, \\ B_y &= \tilde{B}(k_x, k_z)\cos k_x x \cosh k_y y \sin k_z z, \\ B_z &= \tilde{B}(k_x, k_z)\frac{k_z}{k_y}\cos k_x x \sinh k_y y \cos k_z z, \end{aligned}$$

a possible vector potential is:

$$A_x = 0, \tag{69}$$

$$A_y = \tilde{B}(k_x, k_z)\frac{k_z}{k_x k_y}\sin k_x x \sinh k_y y \cos k_z z, \tag{70}$$

$$A_z = -\tilde{B}(k_x, k_z)\frac{1}{k_x}\sin k_x x \cosh k_y y \sin k_z z. \tag{71}$$

In the Polar basis (36)-(38):

$$B_\rho = \tilde{B}_m(k_z) I'_m(k_z\rho) \sin m\theta \cos k_z z,$$

$$B_\theta = \tilde{B}_m(k_z) \frac{m}{k_z\rho} I_m(k_z\rho) \cos m\theta \cos k_z z,$$

$$B_z = -\tilde{B}_m(k_z) I_m(k_z\rho) \sin m\theta \sin k_z z,$$

a possible vector potential is:

$$A_\rho = -\frac{\rho}{m} I_m(k_z\rho) \cos m\theta \sin k_z z, \tag{72}$$

$$A_\theta = 0, \tag{73}$$

$$A_z = -\frac{\rho}{m} I'_m(k_z\rho) \cos m\theta \cos k_z z. \tag{74}$$